

Surface Modification of Low-Carbon Steel via Ferro-Titanium Thermal Diffusion for Enhanced Wear Resistance in Agricultural Machinery



Zahraa Mohammed Dinar*^{ORCID}, Abdul Sameea Jasim Jilabi^{ORCID}, Hayder Abed Hasan Aljuboori^{ORCID}

Department of Metallurgical Engineering, College of Materials Engineering, University of Babylon, Hilla 51001, Iraq

Corresponding Author Email: mat573.zahraa.mohammed@student.uobabylon.edu.iq

Copyright: ©2026 The authors. This article is published by IETA and is licensed under the CC BY 4.0 license (<http://creativecommons.org/licenses/by/4.0/>).

<https://doi.org/10.18280/rcma.360108>

ABSTRACT

Received: 10 December 2025

Revised: 5 February 2026

Accepted: 19 February 2026

Available online: 28 February 2026

Keywords:

low-carbon steel, ferro-titanium, thermal diffusion, titanium carbide, wear resistance, agricultural machinery, cost effectiveness

Agricultural machinery components such as plowshares and harvester blades operate under severe abrasive and impact conditions, necessitating materials with exceptional hardness and wear resistance. While conventional high-carbon steels meet these requirements, their high cost limits widespread use. This study investigates a cost-effective surface modification strategy for low-carbon steel (grade designation of low carbon steel grade (GOST)) employing pack cementation with ferro titanium (Fe-Ti) powder. The treatment produced a composite surface layer consisting of titanium carbide (TiC) reinforced by Fe-Ti intermetallics on a ductile steel substrate. Microstructural characterization via scanning electron microscopy (SEM), energy dispersive X-ray spectroscopy (EDS), and X-ray diffraction (XRD) confirmed the formation of TiC and Fe-Ti phases. Vickers microhardness measurements indicated a surface hardness of 1105 HV, approximately 6.5 times that of the untreated substrate (171 HV). Pin on disc wear tests revealed that the modified surface exhibits wear resistance comparable to that of hardened high carbon steel (grade 65Γ). An economic assessment showed that the proposed process reduces material and processing costs by about 30% relative to conventional high carbon steel components, while also lowering energy consumption and simplifying manufacturing. The results demonstrate that Fe-Ti thermal diffusion is a technically robust and economically viable surface enhancement route for low-carbon steel parts in agricultural applications.

1. INTRODUCTION

The agricultural sector, a cornerstone of the global economy, is critically dependent on machinery and equipment that can withstand extreme operational conditions to meet global food production demands. Components such as plowshares, tines, harvester blades, and threshing teeth are subjected to severe, relentless, abrasive wear from soil, rocks, and plant matter, in addition to significant impact stresses [1]. The service life and efficiency of these machines are directly correlated with the durability of their working parts [2]. Consequently, there is a perpetual demand for materials with exceptional hardness and wear resistance. Traditionally, this requirement has been met by using high-performance, heat-treatable alloys, particularly medium- to high-carbon steels. For example, a widely utilized steel alloy for such applications has a composition of approximately 0.65% C, 0.9-1.2% Mn, and 0.37% Si [3]. This is due to their superior mechanical properties after hardening and tempering, where this material provides a favorable balance of toughness and hardness [4]. However, these specialized alloys are often expensive, contributing significantly to the overall manufacturing cost and making equipment less accessible and more expensive to maintain. Therefore, their relatively high cost poses a

significant economic burden on manufacturers and end-users [5]. The economic necessity of finding cost-effective alternatives without compromising performance has led to intensive research in materials science and agricultural engineering.

Thermal diffusion surface modification presents a promising and cost-effective metallurgical solution. This process involves diffusing alloying elements into the surface of a low-cost substrate, such as low-carbon steel, to create a hard, wear-resistant layer. The use of ferro-titanium (Fe-Ti) powder is particularly attractive for this purpose due to the formation of stable and hard titanium carbides (TiC) on the steel surface, which are known for their exceptional hardness and resistance to abrasive wear. The ability to modify the surface properties of an inexpensive base material allows for the creation of a composite structure: a tough and ductile core for impact resistance, combined with a hard, wear-resistant surface for durability.

This study aims to evaluate the effectiveness of thermal diffusion surface modification of low-carbon steel using Fe-Ti powder as a viable and cost-effective alternative to the conventional use of expensive high-carbon alloys in agricultural engineering. A comprehensive comparison is conducted between the modified low-carbon steel and a

hardened and tempered commercial high-carbon alloy, focusing on key performance indicators. This comparative analysis includes an in-depth examination of the microstructure, coating chemical composition, phase formation, and, most importantly, the resulting hardness and wear resistance. Furthermore, the study includes a thorough analysis of the economic feasibility, comparing the cost of the thermal diffusion process with that of manufacturing components from the expensive high-carbon alloy. The findings of this research will provide valuable insights into the potential of thermal diffusion as a sustainable and economically sound solution for enhancing the performance of agricultural machinery components.

The pursuit of enhancing the surface properties of inexpensive materials, particularly low-carbon steel, has been a key area of research for decades. Surface modification techniques offer a promising pathway by creating a hard, wear-resistant layer on a low-cost, ductile substrate, thereby combining the benefits of a tough core and a durable surface. Among these techniques, thermal diffusion, also known as pack cementation or surface alloying, stands out as a robust and scalable method. This process involves heating the workpiece in a powder mixture containing a source of alloying elements, which then diffuses into the surface of the steel [6].

The use of titanium carbide (TiC) as a surface-hardening agent has been a subject of significant interest in the literature. TiC is a ceramic known for its exceptional hardness (approximately 3200 HV), high melting point, and chemical stability, making it an ideal material for combating abrasive and erosive wear. Numerous studies have demonstrated the successful formation of TiC-rich layers on steel substrates. Some of these studies [7-9] investigated the formation of a TiC layer on AISI 1045 steel using a thermal diffusion method and reported a significant increase in surface hardness and wear resistance. Other studies [10, 11] highlighted the role of process parameters, such as temperature and holding time, in controlling the thickness and morphology of the TiC layer, which directly influences its mechanical performance.

A particularly effective method for introducing titanium is through the use of Fe-Ti powder. Fe-Ti alloys act as a convenient and controlled source of titanium, facilitating the diffusion process and the subsequent formation of TiC. Several studies [11-14] confirmed that using a Fe-Ti powder pack with an appropriate activator can lead to the formation of a dense, uniform titanium carbide layer on low-carbon steel, resulting in a substantial improvement in wear resistance compared to the untreated substrate.

Despite the promising metallurgical outcomes, a comprehensive cost-effectiveness analysis comparing this

surface modification technique with the use of expensive alloys is often lacking in the existing literature. While some studies allude to the economic benefits, a direct, quantitative comparison of manufacturing costs, material costs, and service life is essential for practical industrial adoption. Given the specific demands of the agricultural sector—which prioritize both durability and economic viability—a direct comparison between the performance and cost of a thermally diffused low-carbon steel component and a traditional hardened and tempered high-carbon steel component is critically needed [6].

This paper addresses this gap by providing a detailed comparative evaluation of the two approaches. It will not only present the metallurgical and mechanical properties of the thermally diffused low-carbon steel but will also benchmark these results against those of a commercially used high-carbon steel. The central aim is to demonstrate that thermal diffusion surface modification using Fe-Ti powder is not only a technically sound method for enhancing mechanical properties but also a genuinely cost-effective and viable alternative for manufacturing critical components for agricultural machinery.

Based on the literature review and experimental results, it can be concluded that the use of Fe-Ti powder for surface modification has not been reported in previous studies. Therefore, the present research introduces a new approach for developing hard, wear-resistant coatings on low-carbon steel.

2. EXPERIMENTAL WORK

2.1 Steel alloys

Table 1 exhibits the steel alloys used in the present study according to the Russian State Standard (ГОСТ) [15]. The table involves two kinds of steel alloys. The first one is low-carbon steel (designation of low carbon steel grade (GOST)), which is used as a substrate for thermo-diffusion surface modification. The second steel alloy is the expensive high carbon steel (65Г), the hardenable steel which is commonly used for the manufacturing of agricultural engineering products. The chemical composition analysis in Table 2 presents that the composition (as an average of three readings) of the raw steel alloys falls within the ranges identified by the ГОСТ.

2.2 Coating powder

Table 3 shows the coating powder material used with its chemical composition.

Table 1. Specifications of steel alloys utilized in this research and their elemental composition

| Alloy | Chemical Composition (wt.%) | | | | | Standard Code (ГОСТ) | Raw Material Form and Cross-Section (mm) | Vickers Hardness (HV) | Raw Material Condition |
|-------------------|-----------------------------|---------|-----------|--------|--------|--|--|-----------------------|------------------------|
| | C | Mn | Si max. | P max. | S max. | | | | |
| Low-carbon steel | 0.14-0.22 | 0.4-0.7 | 0.3 | 0.04 | 0.05 | designation of low carbon steel grade (GOST) | rod Ø10 | 125 | Normalized |
| High carbon steel | 0.62-0.7 | 0.9-1.2 | 0.17-0.37 | 0.04 | 0.04 | 65Г | | 218 | Annealed |

Table 2. Analyzed the elemental composition of steel alloys

| Steel Alloy | Elemental Composition (wt.%) | | | | |
|---|------------------------------|-------|-------|--------|-------|
| | C | Mn | Si | P | S |
| Low-carbon steel (designation of low carbon steel grade (GOST)) | 0.276 | 0.493 | 0.162 | 0.0027 | 0.021 |
| High carbon steel (65Г) | 0.64 | 1.04 | 0.26 | 0.028 | 0.03 |

2.3 Pack cementation surface modification

The following procedures have been carefully performed.

- (1) Cutting the raw material of the steel alloys shown in Table 1 (a bar with a diameter of 10 mm) by a lathe machine to produce a 5 mm thick disc ($\text{Ø}10 \times 5$ mm) and a cylindrical specimen with a height of 10 mm ($\text{Ø}10 \times 10$ mm) of low-carbon steel (designation of low carbon steel grade (GOST)). In addition, a cylindrical specimen with a height of 10 mm ($\text{Ø}10 \times 10$ mm) of high carbon steel (65Г) has also been produced.
- (2) The two surfaces of sample cross-sections were ground using a surface grinding machine, washed, and dried. The surfaces were then re-ground in a second stage using sandpaper of various grades (600, 800, 1000), before being washed with ethanol and dried.
- (3) Preparing samples for pack cementation. This was achieved by adding coating powder (Table 3) to a

depth of 10 mm at the bottom of a silica crucible ($\text{Ø}50 \times 70$ mm), then placing the sample made of designation of low carbon steel grade (GOST), before adding the powder; covering it to a depth of 10 mm. The powder was compacted during additions, and a 10 mm fine silt layer of 99.95% alumina (Al_2O_3) was then added before compaction.

- (4) Placing the prepared crucible in an electric oven and heating it gradually to 800°C , then soaking it at that temperature for 2 hours before gradually cooling it to room temperature.
- (5) Removing the sample from the crucible and cleaning it in preparation for subsequent tests.

Table 3. Chemical composition of coating powder

| Coating Powder | Chemical Composition (wt.%) | | | | |
|------------------------|-----------------------------|-------|------|------|------|
| | Fe | Ti | Al | Si | Mn |
| Ferro-titanium (Fe-Ti) | 58.76 | 30.71 | 5.48 | 2.72 | 0.90 |

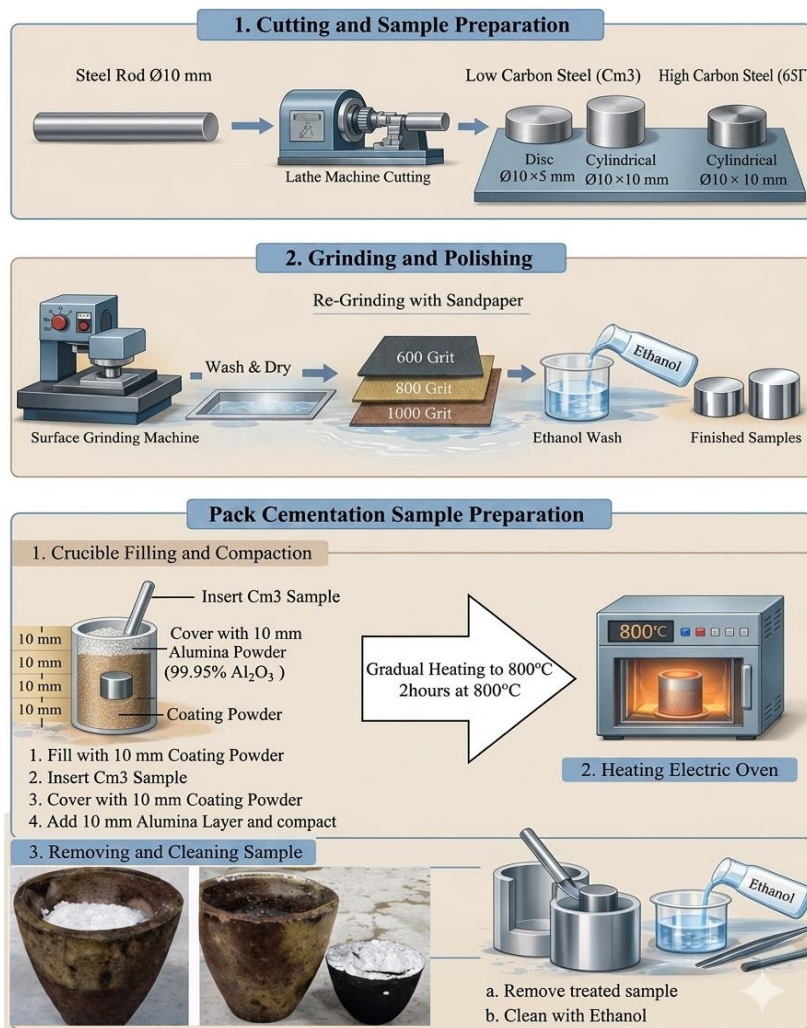


Figure 1. Schematic illustration of the procedures for pack cementation surface modification

Hardening heat treatment of the 65Г steel sample was carried out according to Russian specifications (ГОСТ). This involved gradually heating the sample in an electric oven to 850°C for an hour, then quenching it in oil before washing and drying. The sample was then subjected to a stress-relief annealing process by heating it to 150°C for an hour, followed by gradually cooling to room temperature.

Figure 1 explains the procedures of the pack cementation surface modification technique.

2.4 Microscopy

Specimens for microstructural examination were prepared based on typical metallographic techniques according to ASTM E3-2017 and ASTM E 407-2023 for use with optical microscopy (OM), scanning electron microscopy (SEM), and energy dispersive X-ray spectroscopy (EDS). This is to

recognize the microstructures, topography, and chemical composition of the surfaces. The SEM and EDS examinations were implemented on cross section of the coated specimen, including the coating layer and the substrate, whereas the hardened specimen was examined by the OM. The specimens that were prepared were further employed to examine and characterize the nature, dimensions, and positions of the potential surface flaws.

2.5 X-ray diffraction

This test was conducted to verify the phases and compounds that constitute the coating layer. The X-ray diffraction (XRD) graph was analyzed with the help of analytical cards to explore the different constituents. This test was carried out according to BS EN 13925-1: 2008 and INSO 21951-1-1396. Table 4 shows the most important test conditions.

Table 4. X-ray diffraction (XRD) test conditions

| Current (mA) | Voltage (kV) | Anode | 2θ (°) | Step Size (°) | Counting Time (sec) | Ambient | |
|--------------|--------------|-------|--------|---------------|---------------------|------------|--------------|
| | | | | | | Temp. (°C) | Moisture (%) |
| 30 | 40 | Cu | 2-110 | 0.02 | 0.5 | 23 | 30 |

Table 5. Loads utilized with different materials

| Coated Specimen | | Hardened Specimen |
|-----------------|---|-------------------------|
| Coating Layer | Low-Carbon Steel Substrate (designation of low carbon steel grade (GOST)) Load (grf) | High Carbon Steel (65Г) |
| 10 | 100 | 1000 |

Table 6. The wear test parameters used in this study

| Applied Load (N) | Sliding Radius (mm) | Rotational Speed (r.p.m) | Testing Time (min) | Test Temp. (°C) | Test Moisture (%) | Abrasive Disc Hardness (HV) |
|------------------|---------------------|--------------------------|--------------------|-----------------|-------------------|-----------------------------|
| 2 | 20 | 20 | 90 | 23 | 50 | > 2060 |

2.6 Micro-hardness test

Vickers micro-hardness test was performed on the specimen surfaces, and the substrate metal before treatment. This examination was executed after grinding and polishing the surfaces being measured under different loads (Table 5) for 10s according to ASTM E 384-22, with an average of three measurements per point.

2.7 Wear test

For the wear test, a pin with Ø10 × 10 mm was used with the pin on the disk method. The wear resistance of the coating layer was measured based on weight loss at different sliding distances. The amount of wear depends on the applied force, sliding distance, speed, and environmental conditions of the test procedure shown in Table 6. Subsequently, the specimens were weighed using a digital sensitive balance with 0.0001 g accuracy. This test was done according to ASTM G 99 (2023).

3. RESULTS

SEM coupled with EDS was employed to perform microstructural and elemental analysis of the coating layer

deposited on the designation of low carbon steel grade (GOST) steel substrate. In addition, XRD analysis was conducted to identify the phases and compounds present within the coating.

However, the microstructure of hardened steel (65Г) has been verified by the OM. Hardness and wear resistance tests were also carried out on the samples.

3.1 Microscopic metallography

Figure 2 shows the SEM micrograph of the low-carbon steel (designation of low carbon steel grade (GOST)) substrate before surface treatment. The microstructure consists mainly of a ferrite phase along with pearlite colonies.

The ferrite phase occupies a larger volume fraction compared to the pearlite phase, which is distributed discontinuously within the matrix.

Figure 3 shows the cross-sectional microstructure of the coating layer after the thermal diffusion treatment. The coating exhibits a multi-phase morphology composed of three distinct regions. Region 1 consists of blocky, multifaceted particles uniformly distributed within the coating layer. Region 2 represents the matrix phase surrounding these particles, while Region 3 appears as porous and irregular areas with a complex morphology.

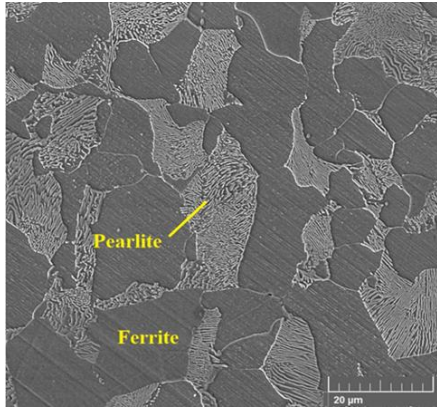


Figure 2. Microstructure of the substrate alloy

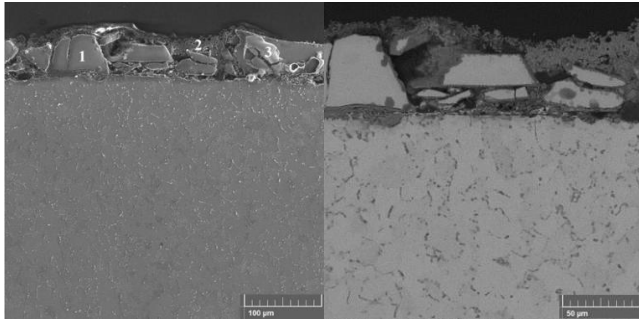


Figure 3. The SEM microstructure of the coating layer with two different magnifications

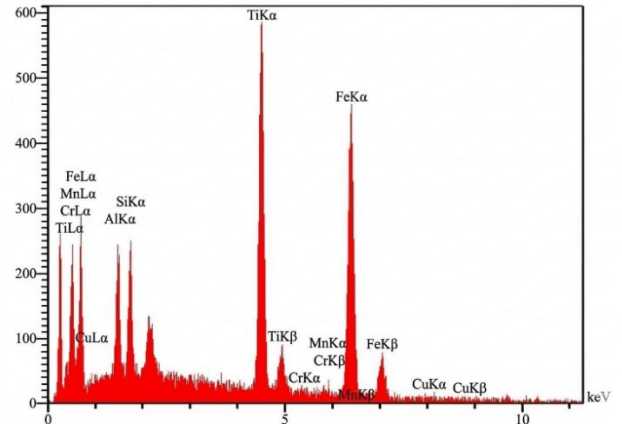


Figure 4. Energy dispersive X-ray spectroscopy (EDS) spectrum of the coating layer

Table 7. Energy dispersive X-ray spectroscopy (EDS) analysis of coating layer (composition in wt.%)

| Element | Fe | Ti | Al | Si | Mn |
|----------------|-------|-------|------|------|------|
| Content (wt.%) | 58.08 | 30.62 | 5.31 | 4.82 | 0.34 |

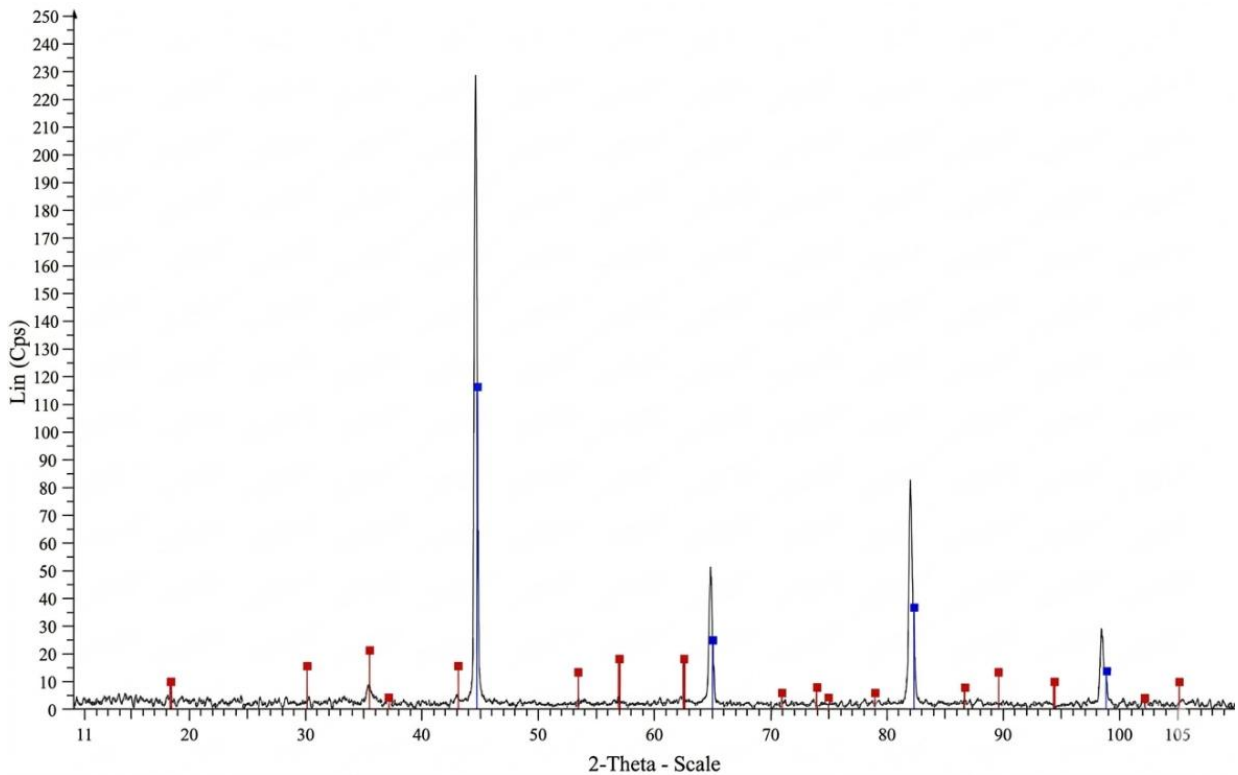


Figure 5. X-ray diffraction (XRD) pattern of the coating surface

Figure 4 presents the EDS spectrum collected from the coating layer. The spectrum shows strong peaks corresponding to TiKα (~4.5 keV) and FeKα (~6.4 keV), indicating that titanium and iron are the major elements present. Weaker peaks corresponding to AlKα (~1.5 keV), SiKα (~1.7 keV), MnKα (~5.9 keV), and CrKα (~5.4 keV) are also detected, suggesting the presence of these elements in smaller quantities, which are consistent with the chemical analysis

shown in Table 7. No significant oxygen peaks are observed in the spectrum.

Figure 5 shows the XRD pattern of the coated sample after the thermal diffusion treatment. Strong diffraction peaks are observed at 2θ values of approximately 44.7°, 64.8°, and 82°, corresponding to the α-Fe (BCC) phase.

Additional diffraction peaks appear at approximately 35.9°, 41.7°, 60.5°, 72.4°, and 76.1°. Several other peaks are detected

near 42°, 44°, 61°, and 77°. The diffraction pattern of the uncoated substrate is dominated by α .

Figure 6 illustrates the surface microstructure of the hardened specimen. The microstructure is mainly composed of martensite, which represents the dominant phase at the surface. No ferrite or pearlite phases are observed in the hardened condition.

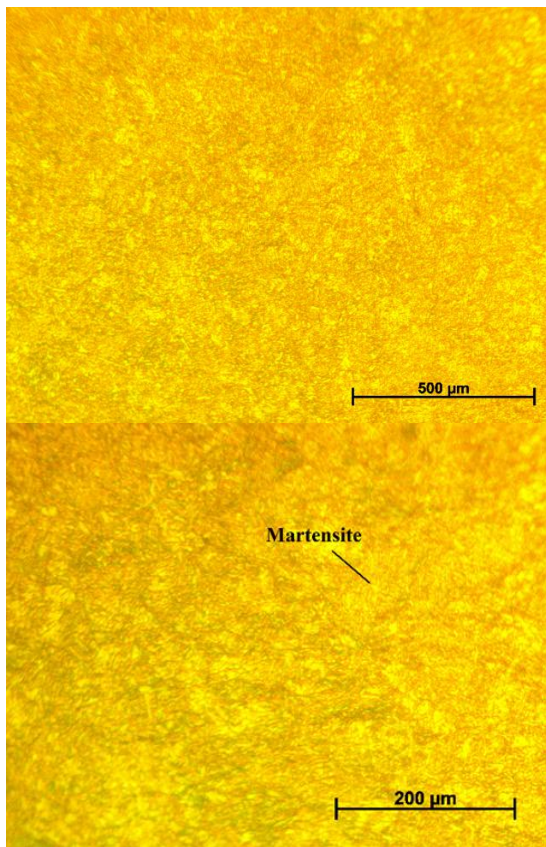


Figure 6. Microstructure of the hardened specimen surface

3.2 Vickers microhardness

The Vickers microhardness results indicate a substantial increase in the average hardness of the coating layer, with a measured value of approximately 1105 HV. This value is approximately 6.5 times the hardness of the designation of low carbon steel grade (GOST) low-carbon steel substrate (171 HV). The hardened steel specimen exhibits a Vickers hardness of approximately 881 HV. This value is about 80% of that of the coating layer.

3.3 Wear resistance

The pin-on-disc wear test results show that the coating layer exhibits a weight loss rate of approximately 0.2×10^{-4} g/min. The hardenable steel sample records a weight loss rate of about 0.83×10^{-5} g/min. These values indicate a difference in wear behavior between the coated layer and the hardenable steel specimen.

3.4 Cost effectiveness

The economic analysis and comparative evaluation of the two surface treatment techniques indicate that the thermal diffusion process using Fe-Ti powder provides a lower overall processing cost compared to the hardened and tempered high-

carbon steel (0.65%C) method.

The total cost reduction associated with the thermal diffusion technique is estimated to range between 25% and 40%. Low-carbon steel (designation of low carbon steel grade (GOST)) substrates are approximately 60% less expensive than high-carbon steel alloys. In addition, components treated by thermal diffusion are estimated to be about 30% less costly than those manufactured entirely from hardened high-carbon steel, while achieving comparable surface hardness and wear resistance.

4. DISCUSSION

4.1 Microscopic metallography

The ferrite-pearlite microstructure observed in the designation of low carbon steel grade (GOST) substrate is typical of low-carbon steels in the normalized condition. The dominance of the ferritic phase is associated with the relatively low carbon content of the alloy.

However, the pearlite fraction observed in Figure 2 appears slightly higher than that typically reported for standard low-carbon steels. This variation can be attributed to the actual carbon content measured in Table 2, which is marginally higher than the nominal composition specified in Table 1. An increase in carbon content promotes pearlite formation, leading to a higher pearlite volume fraction within the ferritic matrix.

The faceted, blocky morphology observed in Region 1 of Figure 3 is characteristic of titanium carbide (TiC), which commonly forms during thermo-diffusion processes when titanium reacts with carbon from the steel substrate. The EDS analysis shown in Table 3 reveals that the Ti content in the coating powder is approximately 30%, which strongly supporting the formation of TiC.

The matrix phase in Region 2 is most likely composed of Fe-Ti intermetallic compounds, such as FeTi or Fe₂Ti, or a titanium-enriched iron solid solution. This interpretation is consistent with the EDS composition of the coating powder, which shows iron as the primary element with a significant titanium content. Such phases typically develop around TiC particles during diffusion-based coating formation.

The irregular and porous features observed in Region 3 may be attributed to partially reacted Fe-Ti particles or the formation of secondary phases. The presence of aluminum and silicon, as indicated by the EDS analysis of the coating powder (Table 3), suggests the possible formation of Ti-Al or Ti-Si intermetallics, while oxide or silicide phases (TiO₂, Al₂O₃, Ti-Si compounds) cannot be completely excluded.

This heterogeneous microstructural configuration is expected to contribute to the enhanced hardness and wear resistance of the coating by combining hard ceramic phases with intermetallic and metallic matrix phases.

The predominance of Ti and Fe peaks shown in Figure 4 supports the formation of titanium-rich phases and Fe-based intermetallics in the coating layer. Minor elements such as Al, Si, Mn, and Cr may contribute to the formation of secondary intermetallic or solid-solution phases, influencing the mechanical and wear properties of the coating.

The absence of significant oxygen peaks indicates that the coating is largely free from oxides. Although carbon is not efficiently detected by EDS due to its weak sensitivity, its contribution is expected since the steel substrate provides

carbon during the diffusion process, facilitating the formation of TiC, which is a hard reinforcing phase in the coating. This composition aligns with the observed enhancement in hardness and wear resistance of the coated layer.

The presence of strong α -Fe diffraction peaks shown in Figure 5 indicates that the base material maintains its BCC structure and a possible Fe(Ti) solid solution, after the thermal diffusion treatment. The appearance of additional diffraction peaks in the coated sample suggests the formation of new phases, indicating evidence of TiC, confirming region 1 in SEM. as a result of the diffusion process. These phases are attributed to the interaction between the substrate and the diffused elements during thermal treatment. Several other peaks suggest possible Fe–Ti intermetallics (Fe₂Ti, FeTi), although partial overlap with TiC and α -Fe complicates precise identification. The overall Fe (~58%) and Ti (~30%) composition supports the presence of these phases in the matrix (Region 2).

No distinct peaks were assigned to Al- or Si-rich compounds (e.g., TiAl, TiSi₂), though their minor presence cannot be excluded, likely corresponding to Region 3 in SEM.

In summary, the coating surface is mainly composed of TiC as the reinforcing phase, supported by α -Fe (substrate/solid solution), and likely Fe–Ti intermetallics, in agreement with SEM–EDS observations. The increased number of diffraction peaks compared to the uncoated substrate confirms the modification of the surface layer through coating formation, which is consistent with the objectives of the thermal diffusion process.

4.2 Vickers microhardness

The significant enhancement in surface hardness observed in the coating layer can be attributed to the formation of hard phases during the treatment process. The exceptionally high hardness value of the coating layer is associated with the presence of titanium carbide (TiC), which is recognized for its superior hardness and reinforcing effect.

In addition, the high hardness measured in the hardened steel specimen is mainly related to the formation of a martensitic microstructure, the dominant constituent as confirmed by the microstructural observations in Figure 6.

Although the hardened steel shows considerable hardness, its value remains lower than that of the coating layer, reaching approximately 80% of the coating hardness. This comparison highlights the superior hardening efficiency of the coating layer over conventional hardening treatment.

4.3 Wear resistance

The wear performance of the coating layer is influenced by its high surface hardness, which contributes to improved resistance against material removal during sliding. Despite having lower hardness than the coating layer, the hardenable steel sample demonstrates a lower weight loss rate, indicating superior wear resistance under the applied test conditions.

This behavior can be attributed to the intrinsic nature of the hardened steel surface, in contrast to the extrinsic coating layer, which may be more susceptible to wear-related damage such as micro-fracture or delamination. Nevertheless, the coated sample still exhibits a reasonable level of wear resistance, demonstrating its effectiveness as a surface modification technique when compared with conventional hardening treatment.

Although agricultural machinery components operate under severe abrasive and impact conditions in real service, a relatively low normal load of 2 N was deliberately selected for the pin-on-disc wear test in the present study. This load was chosen to ensure controlled laboratory conditions that allow the intrinsic wear behavior of the coating layer to be evaluated without inducing premature failure or delamination of the relatively thin diffusion-modified surface.

The objective of the wear test was to provide a comparative assessment of wear resistance between the Fe–Ti thermally diffused low-carbon steel (designation of low carbon steel grade (GOST)) and the conventionally hardened high-carbon steel (65T) under identical testing conditions. The selected load is consistent with ASTM G99 guidelines and has been commonly adopted in laboratory-scale abrasive wear studies to isolate material response and enable reliable comparison of different surface treatments.

Furthermore, using a moderate load enhances the sensitivity of weight-loss measurements, allowing subtle differences in wear mechanisms and coating performance to be clearly distinguished. This approach ensures reproducibility and meaningful comparison while maintaining the structural integrity of the modified surface layer.

4.4 Cost effectiveness

The superior cost-effectiveness of the thermal diffusion process using Fe–Ti powder is primarily related to material selection and processing simplicity. The use of low-carbon steel (designation of low carbon steel grade (GOST)) significantly reduces raw material costs [9], making the process particularly suitable for agricultural equipment components such as plowshares, tines, harvester blades, and threshing teeth [11, 16].

Furthermore, the availability of Fe–Ti and alumina powders from local sources minimizes transportation expenses and supply chain constraints [10, 17]. Unlike the hardened and tempered high-carbon steel route, the thermal diffusion process produces a TiC surface layer that provides high hardness and wear resistance without requiring additional heat treatment steps, such as quenching and tempering. This contributes to reduced processing time, energy consumption, and operational costs [16, 17].

In addition to its economic advantages, the thermal diffusion process aligns with sustainable manufacturing principles by lowering energy requirements and reducing the need for complex equipment, thereby decreasing the overall environmental footprint [18-20].

5. CONCLUSIONS

The economic and technical analysis of surface modification methods indicates that thermal diffusion for low-carbon steel (designation of low carbon steel grade (GOST)) using Fe-Ti powder is the most cost-effective and practical approach for agricultural components such as plows, harvesters, and threshers.

This method provides significant material cost savings, with total costs reduced by approximately 30% compared to hardened and tempered high-carbon steel, while achieving comparable surface hardness and wear resistance.

The thermal diffusion technique also supports environmental sustainability through lower energy

consumption.

Overall, Fe–Ti thermal diffusion is recommended as an efficient and economically viable technique for surface modification of low-carbon steel (designation of low carbon steel grade (GOST)), with optimized operational parameters ensuring maximum mechanical performance at minimal cost.

Recommendations: 1) Using other coating materials, such as ferro-boron. 2) Using an activator with the coating powder. 3) Using different temperatures and times in the thermo-diffusion technique. 4) Conducting corrosion tests under conditions that simulate the operating requirements of agricultural machinery components.

REFERENCES

[1] Malvajerdi, A.S. (2023). Wear and coating of tillage tools: A review. *Heliyon*, 9(6): e16669. <https://doi.org/10.1016/j.heliyon.2023.e16669>

[2] Ikumapayi, O.M., Laseinde, O.T., Ting, T.T. (2024). Mechanical and tribological behaviours of aluminium metal matrix composite reinforced with bamboo powder and iron filings. *Revue des Composites et des Matériaux Avancés-Journal of Composite and Advanced Materials*, 34(4): 447-455. <https://doi.org/10.18280/rcma.340406>

[3] ASM International. Handbook Committee. (1990). Properties and Selection--Irons, Steels, and High-performance Alloys (Vol. 1). ASM International.

[4] Wang, Y., Li, D., Nie, C., Gong, P., Yang, J., Hu, Z., Li, B., Ma, M. (2023). Research progress on the wear resistance of key components in agricultural machinery. *Materials*, 16(24): 7646. <https://doi.org/10.3390/ma16247646>

[5] Ononiwu, N.H., Ozoegwu, C.G., Madushele, N., Akinlabi, E.T. (2021). Machinability and wear resistance improvement in aluminium-based composites 2020. *Revue des Composites et des Matériaux Avancés-Journal of Composite and Advanced Materials*, 31(4): 207-216. <https://doi.org/10.18280/rcma.310404>

[6] Yousef, A., Bastaweesy, A.M., Maaafa, I.M., Abutaleb, A. (2024). Improved surface properties of low-carbon steel by chromizing-titanizing coating using pack cementation process. *Metals*, 14(12): 1456. <https://doi.org/10.3390/met14121456>

[7] Saroj, S., Sahoo, C.K., Masanta, M. (2017). Microstructure and mechanical performance of TiC-Inconel825 composite coating deposited on AISI 304 steel by TIG cladding process. *Journal of Materials Processing Technology*, 249: 490-501. <https://doi.org/doi:10.1016/j.jmatprotec.2017.06.042>

[8] Sharifitabar, M., Khaki, J.V., Sabzevar, M.H. (2016). Microstructure and wear resistance of in-situ TiC-Al₂O₃ particles reinforced Fe-based coatings produced by gas tungsten arc cladding. *Surface and Coatings Technology*, 285: 47-56. <https://doi.org/10.1016/j.surfcoat.2015.11.019>

[9] Ke, S.R., Xu, X.H., Xiang, Z.D. (2015). Feasibility of cladding Ti to carbon steel by diffusion bonding followed by hot-rolling. In 5th International Conference on Advanced Design and Manufacturing Engineering, pp. 1961-1965. <https://doi.org/10.2991/icadme-15.2015.363>

[10] Mao, Z.L., Yang, X.J., Zhu, S.L., Cui, Z.D., Lu, Y. (2014). Pack cementation processing parameters for SiC coatings on C/C for optimum tribological properties.

Surface and Coatings Technology, 254: 54-60. <https://doi.org/10.1016/j.surfcoat.2014.05.060>

[11] Treu, B.L., Fahrenholtz, W., O'Keefe, M., Morris, E., Albers, R. (2011). Effect of phase on the electrochemical and morphological properties of praseodymium-based coatings. *ECS Transactions*, 33(35): 53. <https://doi.org/10.1149/1.3577753>

[12] Zhang, J., Li, S., Lu, C., Sun, C., et al. (2019). Anti-wear titanium carbide coating on low-carbon steel by thermo-reactive diffusion. *Surface and Coatings Technology*, 364: 265-272. <https://doi.org/10.1016/j.surfcoat.2019.02.085>

[13] Liu, Z., Zhao, X., Zhou, C. (2015). Improved hot corrosion resistance of Y-Ce-Co-modified aluminide coating on nickel base superalloys by pack cementation process. *Corrosion Science*, 92: 148-154. <https://doi.org/10.1016/j.corsci.2014.11.043>

[14] Sartwell, B.D., Baldwin, D.A., Singer, I.L. (1985). Effects of pressure and temperature on implantation-induced carburization of steels. *Journal of Vacuum Science & Technology A*, 3(3): 589-590. <https://doi.org/10.1116/1.572956>

[15] Metallurgy Handbook (MH). (1978). Metallurgy Handbook, Prom Import Raw Material, USSR.

[16] Günen, A., Soyulu, B., Karakaş, Ö. (2022). Titanium carbide coating to improve surface characteristic, wear and corrosion resistance of spheroidal graphite cast irons. *Surface and Coatings Technology*, 437: 128280. <https://doi.org/10.1016/j.surfcoat.2022.128280>

[17] Dudziak, T.P., Rząd, E., Medvedovski, E., Mendoza, G.L. (2021). Sulfidation-oxidation resistance of thermal diffusion multi-layered coatings on steels. *Materials*, 14(19): 5724. <https://doi.org/10.3390/ma14195724>

[18] Jędrzejczyk, D., Skotnicki, W. (2021). Comparison of the tribological properties of the thermal diffusion zinc coating to the classic and heat treated hot-dip zinc coatings. *Materials*, 14(7): 1655. <https://doi.org/10.3390/ma14071655>

[19] Peng, L., Sun, Y., Zhang, F., Luan, B. (2025). A study of interface microstructure and mechanical properties of industrial-scale hot-rolled titanium/steel clad plates. *Journal of Alloys and Compounds*, 1036: 181637. <https://doi.org/10.1016/j.jallcom.2025.181637>

[20] James, A.S., Thomas, K., Mann, P., Wall, R. (2005). The role and impacts of surface engineering in environmental design. *Materials & Design*, 26(7): 594-601. <https://doi.org/10.1016/j.matdes.2004.08.011>

NOMENCLATURE

wt. Weight percentage, %

Chemical symbols

| | |
|--------------------------------|---|
| Fe–Ti | Ferro-titanium |
| TiC | Titanium carbide |
| Al ₂ O ₃ | Alumina (aluminum oxide) |
| Fe ₂ Ti | Iron titanium intermetallic compound |
| Fe(Ti) | Iron-based solid solution with dissolved titanium |
| α-Fe | Ferrite (body-centered cubic iron) |
| C _T 3 | Designation of low carbon steel grade (GOST) |
| 65T | Designation of high carbon steel grade |

| | | | |
|----------------------|-----------------------------------|------|---|
| | (GOST) | ASTM | American standards for testing of materials |
| | | BCC | Body-centered cubic |
| Greek symbols | | EDS | Energy Dispersive X-ray Spectroscopy |
| | | HV | Vickers hardness |
| ∅ | Specimen diameter, mm | OM | Optical microscopy |
| Subscripts | | SEM | Scanning electron microscopy |
| | | XRD | X-ray diffraction |
| AISI | American iron and steel institute | | |